

OPTIMAL ATTITUDE CONTROL FOR COPLANAR ORBIT PHASING TRANSFERS

Christopher D. Hall * and I. Michael Ross[†]

We pose and obtain solutions for a class of optimal coplanar orbital maneuvers, in which the spacecraft is controlled to move ahead of or behind its orbit position or to change orbits using a constant thrust whose direction is a control variable. The optimality criterion is a convex combination of three performance indices including time, fuel, and control torque requirements. These optimal orbital maneuvers are conceptually simple. A unique feature of the present work, however, is that we include the attitude control required for steering the spacecraft to achieve the required thrust direction. Thus the attitude dynamics and orbit dynamics are coupled. We illustrate several solutions and discuss the differences between these solutions and those obtained when the spacecraft is modelled as a point mass. Specifically, the angular momentum of the spacecraft can lead to optimal orbital maneuvers in which the thrust vector changes directions in a manner which is significantly different from that found for point-mass spacecraft.

INTRODUCTION

We investigate a special class of coplanar optimal orbital maneuvers, in which the spacecraft is controlled to move ahead of or behind its orbit position using a constant thrust whose direction is the control variable. The minimum-time orbital phasing maneuver is conceptually simple, but its solution has some interesting characteristics, including an approximate invariance relating the dimensionless thrust, phase angle, dimensionless time-of-flight, and thrust profile when the maneuver occurs in less than about one orbit.

The minimum-time, constant-thrust, orbit transfer problem is well-established as one of the fundamental problems in control of spacecraft trajectories.¹⁻³ The problem and its variants are frequently used to benchmark new methods and ideas on optimal control.⁴⁻⁷ Extremals to the problem are those solutions that satisfy the first-order necessary conditions. A recently published procedure is now available for applying second-order necessary conditions,⁸ and another scheme to validate and compute neighboring optimal solutions⁹ for closed-loop guidance. Although these developments are not used in this paper, we verify the finite second-order Legendre-Clebsch condition associated with the convexity of the Hamiltonian. Many applications of this problem involve low-thrust propulsion systems where the

*Professor, Department of Aerospace and Ocean Engineering, Virginia Polytechnic Institute and State University, Blacksburg, Virginia. cdhall@vt.edu. Associate Fellow AIAA, Member AAS.

[†]Associate Professor, Department of Aeronautics and Astronautics, Naval Postgraduate School, Monterey, California 93943. Associate Fellow AIAA. Member AAS. imross@nps.navy.mil. voice: (831) 656-2074.

orbit transfer takes place over a relatively long duration. For example, the minimum-time transfer of a 100 kg spacecraft from low-Earth orbit (LEO) to geostationary orbit (GEO) using a 1 N thruster takes about 5 days, as compared with about 5 hours for a Hohmann transfer, but the continuous-thrust case would typically use much less propellant.

The thrust angle profile of a continuous thrust orbit transfer depends on both the thrust magnitude and the “size” of the orbit transfer. For example, Ref. 10 showed that there are problems involving small orbit changes using low thrust that are similar to large-thrust problems with larger orbit changes. In Ref. 11 the effects of thrust magnitude on trajectory behavior were described in some detail.

The development in Refs. 10 and 12 led to the identification of three different regimes of minimum-time, constant-thrust, coplanar orbit transfer problems, along with a means of approximating the initial conditions on the costates required to determine the extremal control history. In an application of these approximations, Ref. 13 used piecewise time-optimal transfers to investigate the effectiveness of using energy storage during eclipse for low-thrust electric propulsion systems.

In the present paper, we consider optimizing orbital phasing maneuvers using constant thrust with the thrust angle as a state. Specifically, we pose and obtain solutions to the problem of moving a point-mass spacecraft from one point in a given circular orbit to a different point in the same orbit, differing only by a phase angle ϕ . This problem is of course the same as the same-orbit rendezvous problem. However, our motivation is not rendezvous, but rather the formation-establishment and formation-keeping maneuvers associated with formation flying missions.^{14–16} We want to compute minimum-time solutions for comparison with nonlinear feedback controllers^{17–19} designed to support such missions.

We begin by defining the coupled attitude and orbit equations of motion. The equations are non-dimensionalized so that the dimensionless thrust, T , dimensionless inertia, I , the dimensionless mass flow rate, c , and the phase angle, ϕ , are the only parameters in the problem. We then define a three-parameter family of optimal control problems where the parameters form a standard convex combination of the individual cost functionals. The necessary conditions are described along with the second-order condition on the convexity of the Hamiltonian. These necessary conditions are largely used to validate the solutions obtained from DIDO,²⁰ a software package that implements a sparse version⁶ of the Legendre pseudospectral method.²¹ Following a brief description of the methods employed, we present results for several different thrust magnitudes and phase angles.

MODEL AND EQUATIONS OF MOTION

We make the idealized assumptions of a rigid spacecraft moving in a plane about a spherical primary, and being controlled with a constant thrust with variable direction. Figure 1 illustrates the geometry and variables of the problem. The thrust angle, ψ , is defined with respect to the inertial x axis. Additionally, we define the thrust angle relative to the local horizontal as $\bar{\psi}$. In Fig. 1, an arbitrary intermediate configuration is shown, after time $t - t_0$. A reference spacecraft position is shown as a light shaded circle on the circular orbit, whereas the maneuvered spacecraft position is shown as a darker shaded circle removed from the circular orbit. The target position and the uncontrolled spacecraft position have both advanced through an angle $n(t - t_0)$, where n is the mean motion of the

circular orbit. We also indicate the thrust angle referenced to the local horizontal, denoted by $\bar{\psi} = \psi - \theta - \pi/2$.

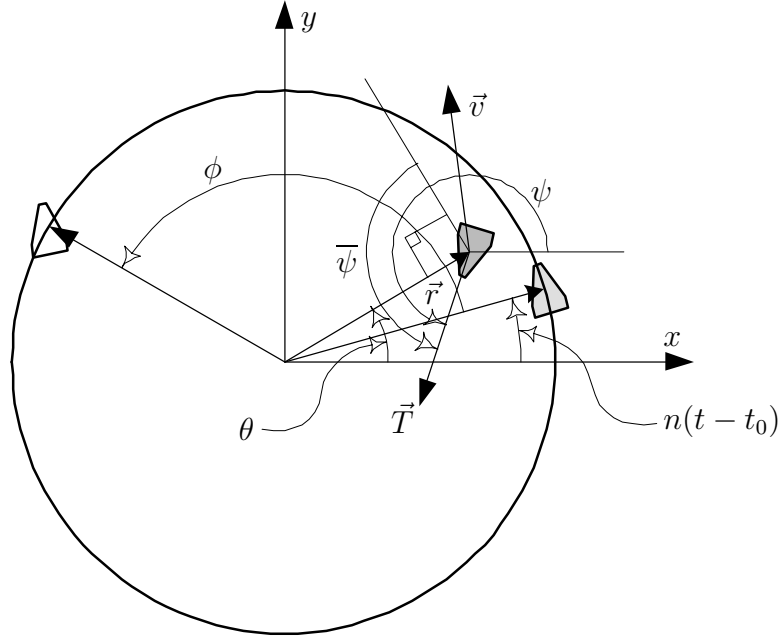


Figure 1: Optimal phasing maneuver geometry

The equations of motion are those for Keplerian motion in the plane, with additional acceleration terms due to the thruster. We assume the spacecraft has constant mass for the results presented in the paper. Using cartesian coordinates in the inertial reference frame shown in Fig. 1, the equations of motion are

$$\dot{x}^* = v_x^* \quad (1)$$

$$\dot{y}^* = v_y^* \quad (2)$$

$$\dot{v}_x^* = -\frac{\mu^*}{r^{*3}}x^* + \frac{T^*}{m^*}\cos\psi \quad (3)$$

$$\dot{v}_y^* = -\frac{\mu^*}{r^{*3}}y^* + \frac{T^*}{m^*}\sin\psi \quad (4)$$

$$\dot{\psi}^* = h^*/I^* \quad (5)$$

$$\dot{h}^* = g^* \quad (6)$$

$$\dot{m}^* = c^* \quad (7)$$

where x^* and y^* are the components of the position vector in the orbital plane, $r^* = \sqrt{x^{*2} + y^{*2}}$, μ^* is the gravitational parameter, ψ is the thrust angle measured from an inertial x -axis, T^* is the applied thrust, m^* is the spacecraft mass, and c^* is the mass flow rate. The spacecraft angular momentum about its mass center is h^* , and its moment of inertia about the pitch axis is I^* . The superscript $*$ denotes dimensional parameters and variables. Using dimensional variables requires that we consider the effects of varying orbit size, thrust magnitude, and spacecraft mass and moment of inertia. Non-dimensionalizing the equations reduces the problem to one with only dimensionless thrust, inertia, and mass flow rate as parameters.

Non-dimensionalization is partially based on canonical units,²² so that the reference orbit semi-major axis is 1 DU (Distance Unit), the reference orbit period is 2π TU (Time Units), and the gravitational parameter is $\mu = 1 \text{ DU}^3/\text{TU}^2$. The initial spacecraft mass, m^* , is taken as the dimensionless mass unit, and it follows that a dimensionless thrust can be defined by

$$T = \frac{T^*}{m^* a^* n^{*2}} \quad (8)$$

where a^* is the reference orbit semi-major axis and n^* is the reference mean motion in dimensional units. Thus, for example, a 1 N thruster acting on a 100 kg spacecraft in a 10,000 km radius circular orbit provides a dimensionless thrust of about $T = 0.0025$. In results illustrated below, we use the range $[0.000005, 0.5]$ as a practical limit on the range of thrusts of interest for this application. For a 100 kg spacecraft, this range corresponds to approximately [4 mN, 400 N] in LEO and [100 μ N, 10 N] in GEO. Even smaller thrusts may be of interest, but the near-invariance described below can be used to obtain results for smaller thrusts in a straightforward way. The expression for T can also be written as

$$T = \left(\frac{T^*}{m^*} \right) / \left(\frac{\mu^*}{a^{*2}} \right) \quad (9)$$

so that T can be interpreted as the ratio of “thrust acceleration” to gravitational acceleration.

Setting $c = 0$, the form of the dimensionless equations is identical to that of the dimensional equations, with the asterisks omitted, and both μ and m set to unity. Thus the dimensionless states are $(x, y, v_x, v_y, \psi, h)$, and the only parameters remaining in the equations of motion are the dimensionless thrust magnitude, T and the dimensionless inertia, I . The other non-state variable in the equations of motion is the control torque g , which is the control variable to be determined.

PROBLEM FORMULATION AND SOME NECESSARY CONDITIONS

We define a Bolza cost functional as

$$J = -w_m m(t_f) + \int_0^{t_f} (w_t + w_u u^2(t)) dt \quad (10)$$

where w_m , w_t , and w_u are weights chosen to explore the convex combination of the individual performance indices by constraining them as,

$$w_m + w_t + w_u = 1 \quad w_m \geq 0, w_t \geq 0, w_u \geq 0 \quad (11)$$

The other variables are u , the control, and t_f , the final time. Choosing different weights and different variables for the control u leads to a family of optimization problems. A sequence of problems of interest may be enumerated as

- P1. Point-mass minimum-time phasing maneuvers. $u = \psi$, with $w_m = w_u = 0$, $w_t = 1$
- P2. Point-mass minimum-time, minimum-fuel phasing maneuvers. $u = \psi$, with $w_m \geq 0$, $w_t = 1 - w_m \geq 0$, $w_u = 0$
- P3. Rigid body minimum-time, L^2 minimum-angular momentum phasing maneuvers. $u = h$, with $w_m \geq 0$, $w_t \geq 0$, $w_u > 0$

- P4. Rigid body minimum-time, L_2 minimum-torque phasing maneuvers. $u = g$, with $w_m \geq 0$, $w_t \geq 0$, $w_u > 0$

Problem 1 was studied extensively in Ref. 23. A version of Problem 3 as it pertains to Solar Sail attitude dynamics is discussed in Ref. 24. To our knowledge, Problem 4 has not received any attention in the literature. In any case, a systematic analysis of the entire family of problems posed above has not been discussed in the literature.

The minimum-time formulation (P1) is well-known and may be found for example in Refs. 1, 2, 3, and 10. The formulation leads to four adjoint differential equations that describe the costates. Making use of the fact that $\mu = 1$ in the dimensionless system, these four differential equations are:

$$\dot{\lambda}_x = \frac{\lambda_{v_x}}{r^3} - \frac{3x}{r^5} (x\lambda_{v_x} + y\lambda_{v_y}) \quad (12)$$

$$\dot{\lambda}_y = \frac{\lambda_{v_y}}{r^3} - \frac{3y}{r^5} (x\lambda_{v_x} + y\lambda_{v_y}) \quad (13)$$

$$\dot{\lambda}_{v_x} = -\lambda_x \quad (14)$$

$$\dot{\lambda}_{v_y} = -\lambda_y \quad (15)$$

that can, in principle, be integrated simultaneously with the state equations (1–4). However, due to well-known stability problems associated with integrating the state-adjoint pair in either direction,² we explore optimal maneuvers by the Legendre pseudospectral method²⁵ that exploits the Covector Mapping Theorem (CMT)²¹ in the software package DIDO.²⁰ For problems P2–P4, additional costate equations are required for indirect methods, but are omitted here, as we use direct methods.

From the stationarity of the Hamiltonian, the thrust angle for problem P1 is given by,

$$-\lambda_{v_x} \sin \psi + \lambda_{v_y} \cos \psi = 0 \quad (16)$$

If this angle is substituted for the control in Eqs. (3–4), it establishes a two-point boundary value problem wherein the initial conditions on the costates are the unknowns. However, as noted above, we circumvent the problems associated with solving the boundary-value problem and instead compute ψ using Eq. (16) and the costates obtained from the CMT. These are our CMT controls, ψ_{CMT} . Following Ref. 26, we declare extremality if $\|\psi_{CMT} - \psi_{DIDO}\| \leq \varepsilon$ where ε is an arbitrarily set convergence tolerance. Here ψ_{DIDO} denotes the controls obtained from DIDO.

The convexity of the Hamiltonian can be checked (by way of the CMT) from the second-order condition,

$$\lambda_{v_x} \cos \psi + \lambda_{v_y} \sin \psi \leq 0 \quad (17)$$

which, if $\lambda_{v_x} \neq 0$, simplifies to,

$$\frac{\cos \psi}{\lambda_{v_x}} \leq 0 \quad (18)$$

over the extremal control. Hence, the convexity of the Hamiltonian may be verified by the binary test,

$$\text{sgn}(\lambda_{v_x}) + \text{sgn}(\cos \psi) = 0 \quad (19)$$

If $\lambda_{v_x} = 0$, then $\psi = \pi/2$ if $\lambda_{v_y} \neq 0$.

For the phasing maneuver considered here, the initial conditions for the orbit states are $x = 1$, $y = 0$, $v_x = 0$, and $v_y = 1$, corresponding to a circular orbit with radius 1 DU beginning on the x axis. The final conditions that the states must satisfy include that the spacecraft must return to the same circular orbit: *i.e.*, $x^2 + y^2 = 1$, $v_x^2 + v_y^2 = 1$, and $xv_x + yv_y = 0$. In addition to these three conditions, we also have the condition corresponding to completion of the phasing maneuver through angle ϕ . Another way to formulate the final conditions on the states is

$$x(t_f) = \cos(\phi + t_f) \tag{20}$$

$$y(t_f) = \sin(\phi + t_f) \tag{21}$$

$$v_x(t_f) = -\sin(\phi + t_f) \tag{22}$$

$$v_y(t_f) = \cos(\phi + t_f) \tag{23}$$

where t_f is the time-of-flight, which is also unknown. An added benefit of the non-dimensionalization is that t_f is the angle the target moves through during the maneuver.

Selection of appropriate boundary conditions for the attitude is less straightforward. Clearly, these could be free variables in the optimization. In the simulation results presented here, we take the initial attitude to be defined by fixing ψ and setting $h = 0$, and leaving the final attitude free.

OVERVIEW OF THE NUMERICAL TECHNIQUE

Numerical methods to solve optimal control problems have been described as direct or indirect methods.²⁹ In indirect methods, the associated two-point boundary value problem is solved by a variety of techniques. In direct methods, the problem is discretized by a variety of techniques and the discrete problem is then solved by yet another variety of techniques. Since direct methods do not automatically tie the resulting solution to the Minimum Principle, in contrast to the indirect methods, the conventional wisdom is that indirect methods are more accurate than direct methods. However, indirect methods come with all the trap-pings described in detail in Ref. 29, one of the most egregious of which is a fundamental stability problem.² In modern terminology, direct methods can be considered as discretizing first and dualizing afterwards while indirect methods reverse the operation.³⁰ In general, these operations are not commutative resulting in a “gap.” The gap can be closed by way of Closure Conditions over a set of convergent methods. The Closure Conditions consequently render a family of “direct” methods just as accurate as the corresponding “indirect” method. Examples of these families of methods are the Runge-Kutta-Hager methods⁵ and the Legendre pseudospectral methods.²¹ An important feature of these “complete” methods is that they satisfy a Covector Mapping Principle (CMP).^{30,31} According to the CMP, there exists a bijective transformation between the Lagrange multipliers associated with the dualization of the discrete problem and the discretization of the dualized problem. A Covector Mapping Theorem (CMT)²¹ is a particular version of the CMP that has been obtained for the Legendre PS method and implemented in the software package DIDO.²⁰ Thus, the results reported in the following section exploit recent advances in nonlinear optimal control theory and techniques to systematically analyze the three-parameter family of orbit transfer problems posed earlier.

EXAMPLE SOLUTIONS

In this section we present several examples of solutions to the posed optimization problem, P4. The examples illustrate the nature of solutions to the optimal control problem with varying thrust T and phase angle ϕ , while holding inertia I constant. For each example we provide plots of the trajectory and the thrust angle relative to the local horizontal. As noted in the previous section, all trajectories begin with initial conditions $x = 1$, $y = 0$, $v_x = 0$, $v_y = 1$, $h = 0$. The initial condition for ψ is chosen either to be zero or to be “close” to the initial thrust angle obtained for the corresponding point-mass problem. Figure 2 illustrates the thrust angle profiles for a wide range of trajectories for problem P1. These profiles, taken from Ref. 23, illustrate four different classes of phasing maneuvers, parameterized by the relationship between thrust magnitude and phase angle. The data for these maneuvers is included in Table 1.

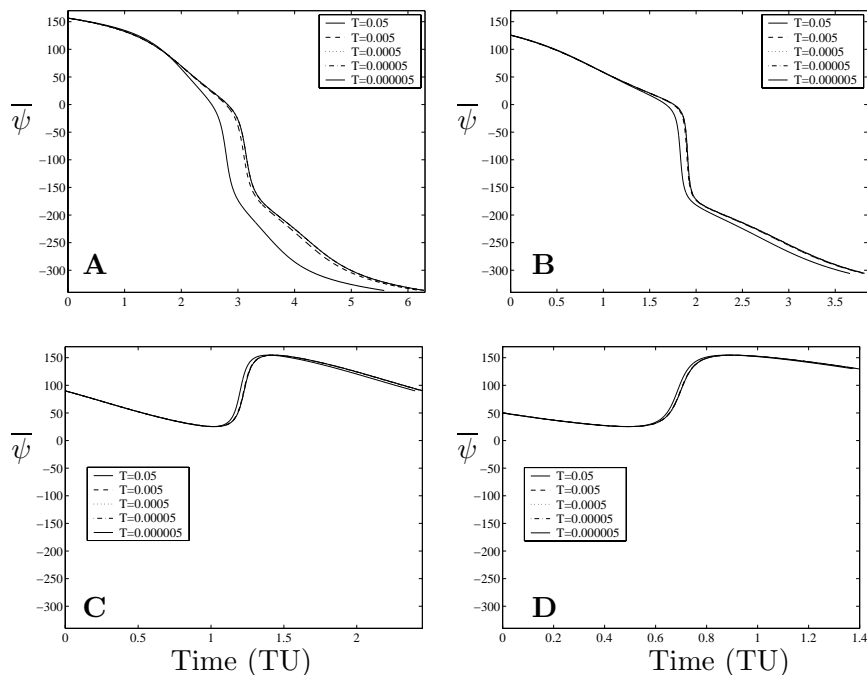


Figure 2: Thrust angle $\bar{\psi}$ for points A, B, C, D of point-mass solutions²³

For cross-reference, see Figs. 5 and 6 of Ref. 23. The latter is reproduced here, and illustrates the thrust angle for four different types of trajectories, labelled A, B, C, and D. As described in detail in Ref. 23, these points represent five orders of magnitude in thrust T and five orders of magnitude in phase angle ϕ . Within each type of trajectory, all have approximately the same time of flight t_f , and approximately the same thrust angle profile, as is evident in Fig. 2.

The first example, Fig. 3, is chosen to correspond to a point-mass problems for which the initial thrust vector is nadir-pointing. This class of points is labelled ‘C’ in Fig. 2 and Table 1. As is evident from the figure and table, the time of flight for these point-mass trajectories is approximately 2.4 TU, and the initial thrust angle is $\bar{\psi} = \pi/2$. During the maneuver, the thrust angle decreases to a value close to, but greater than, zero, and then

Table 1: Data for specific classes of point-mass solutions²³

Point	T	ϕ	$\lambda_y(0)$	$\lambda_{v_x}(0)$	$\lambda_{v_y}(0)$	t_f
A	0.5	—	—	—	—	—
	0.05	0.89	0.34	0.43	1.0	5.6
	0.005	0.10	0.33	0.44		6.2
	0.0005	0.010	0.33	0.44		6.3
	0.00005	0.0010	0.33	0.44		6.3
	0.000005	0.00010	0.33	0.44		6.3
B	0.5	1.46	0.47	0.63	0.5	2.8
	0.05	0.21	0.44	0.69		3.7
	0.005	0.022	0.44	0.70		3.8
	0.0005	0.0022	0.44	0.70		3.8
	0.00005	0.00022	0.44	0.70		3.8
	0.000005	0.000022	0.44	0.70		3.8
C	0.5	0.54	0.14	0.67	0.0	2.0
	0.05	0.071	0.18	0.73		2.4
	0.005	0.0074	0.18	0.73		2.4
	0.0005	0.00074	0.19	0.73		2.4
	0.00005	0.000074	0.19	0.73		2.4
	0.000005	0.0000074	0.19	0.73		2.4
D	0.5	0.17	-0.75	0.53	-0.5	1.2
	0.05	0.022	-0.61	0.60		1.4
	0.005	0.0023	-0.60	0.60		1.4
	0.0005	0.00023	-0.59	0.60		1.4
	0.00005	0.000023	-0.59	0.60		1.4
	0.000005	0.0000023	-0.59	0.60		1.4

has a rapid increase to nearly π and then decreases again. This rapid increase in $\bar{\psi}$ motivates the $w_u u(t)^2$ term in the cost functional, Eq. (10). For a large spacecraft, a rapid attitude maneuver may be expensive in control torque as well as in mitigation of vibrations excited by the maneuver.

In Figure 3, we illustrate a solution obtained using DIDO for the conditions corresponding to the second row of ‘C’ cases in Table 1, with $T = 0.05$, $\phi = 0.073$ and $t_f = 2.4$. To compute the solution to the rigid body problem with attitude control, we select weights $w_t = w_u = 0.5$, with $u = g$. We use the circular orbit initial conditions and set $\psi_0 = \pi(\bar{\psi}_0 = \pi/2)$, $h = 0$. These conditions lead to a phasing maneuver trajectory that takes about 13 TU to complete, more than five times the time required to complete the point-mass phasing maneuver.

The trajectory is graphed in Fig. 3a, with the initial point indicated with a \times and the final point indicated with a \circ . Along the trajectory the thrust direction is illustrated with arrows, and the thrust angle is graphed in Fig. 3b. It is useful to compare this graph with the corresponding graph in Fig. 2C. Whereas the point-mass trajectory reverses direction near the midway point of the trajectory, the rigid body trajectory continues to rotate until the trajectory is about 2/3 complete. This trend is due to the rotational inertia of the spacecraft generated during the initial pointing changes. As the spacecraft inertia is decreased or the

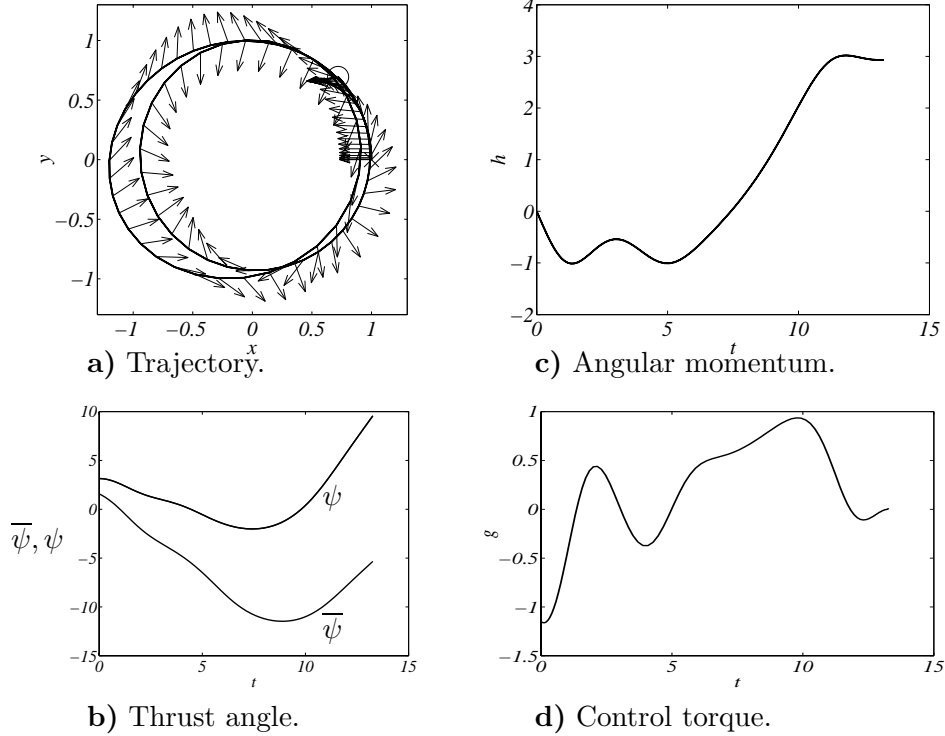


Figure 3: Trajectory, thrust angle, angular momentum, and control torque for Case C2.

control weight w_u is decreased, this trajectory becomes similar to that for the point-mass case.

The second example, illustrated in Fig. 4, is also from the ‘C’ set of cases, but for a smaller thrust and smaller phase angle ($T = 0.005$, $\phi = 0.0073$). This trajectory is similar to that of Fig. 3, but due to the smaller thrust, the trajectory is closer to the nominal circular orbit. Note also that the time-of-flight for this case is nearly identical to that for Case C2.

The next two examples correspond to the set of point-mass problems for which the initial thrust vector opposes the velocity vector direction and is about 50° “below” the horizon direction. These points are labelled ‘B’ in Fig. 2 and Table 1, and the time of flight for the point-mass trajectories is about 3.8 TU. For the rigid body trajectories, we take the initial pointing direction to be in the velocity vector direction; *i.e.*, $\psi_0 = \pi/2$, $\bar{\psi}_0 = 0$. Clearly this choice is not optimal, but it illustrates how the control moves the thrust vector in the rearward direction. The trajectory takes almost 15 TU to complete.

A second example from the ‘B’ set of points illustrates a substantially different trajectory, and shows how the time-invariance of the point-mass problems does not persist for the rigid body problems. In this example, illustrated in Fig. 6, the spacecraft begins to rotate in a clockwise direction and continues to rotate throughout the maneuver, which takes less than 8 TU.

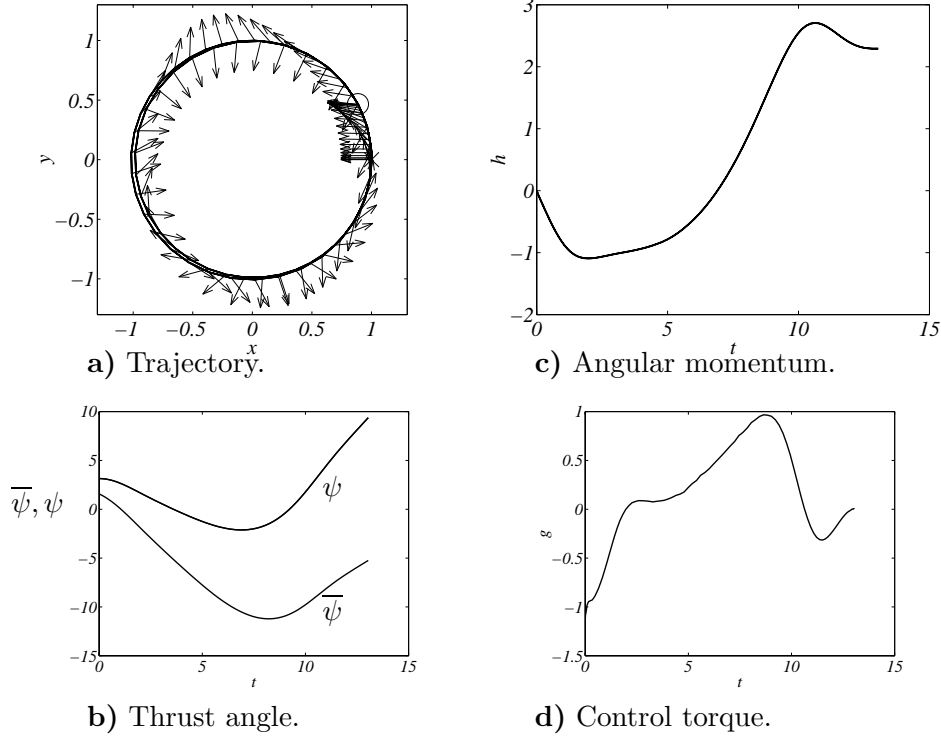


Figure 4: Trajectory, thrust angle, angular momentum, and control torque for Case C3.

The final four cases illustrate trajectories corresponding to point-mass trajectories for which the initial thrust direction is nearly in either the positive or negative velocity direction. For the point-mass cases, initial thrusting in the velocity direction occurs when the thrust-to-phase angle ratio is large, and initial thrusting in the negative velocity direction occurs when the thrust-to-phase angle ratio is small. A simplistic way to view this result is that the best strategy for a large-thrust spacecraft going a short distance is to thrust directly towards the target and reverse thrust direction about halfway there, whereas for a small-thrust spacecraft going a long distance, the best strategy is to lower the orbit and catch up with the target, reversing the thrust direction to raise the orbit about halfway there.

The example in Fig. 7 corresponds to $T = 0.05$, $\phi = 0.89$, and for the point-mass case, the time-of-flight is 5.6 TU. We begin with the attitude thrusting directly forward (approximately opposite the optimal thrust direction for the point-mass case). As with the example in Fig. 6, the spacecraft begins to rotate in a clockwise direction and continues to rotate throughout the maneuver, which takes about 7.5 TU.

The example in Fig. 8 corresponds to $T = 0.5$, $\phi = 0.17$, and for the point-mass case, the time-of-flight is 1.2 TU. We begin with the attitude thrusting directly forward (approximately the same as the optimal thrust direction for the point-mass case). Here the large thrust immediately begins to increase the size of the orbit, and the spacecraft rotates in a counterclockwise direction throughout the maneuver, which takes about 6 TU.

The example in Fig. 9 corresponds to $T = 0.05$, $\phi = 0.022$, and for the point-mass

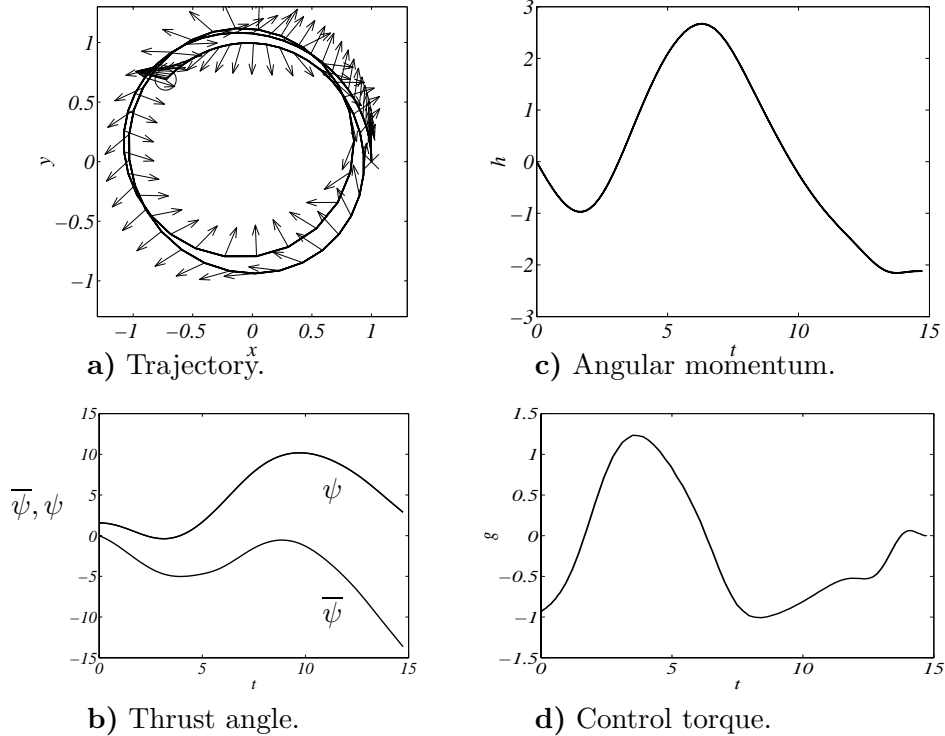


Figure 5: Trajectory, thrust angle, angular momentum, and control torque for Case B2.

case, the time-of-flight is 1.4 TU. We begin with the attitude thrusting directly forward (approximately the same as the optimal thrust direction for the point-mass case). Here the spacecraft begins to rotate in a counterclockwise direction and changes direction about 1/3 of the way through the maneuver, which takes about 6 TU.

The final example, illustrated in Fig. 10 corresponds to $T = 0.005$, $\phi = 0.0022$, and as with the previous example has a point-mass time-of-flight of 1.4 TU. We begin with the attitude thrusting directly forward (approximately the same as the optimal thrust direction for the point-mass case). The trajectory is strikingly different from that of Fig. 9. Here the spacecraft rotates several times during the maneuver, which takes about 5 TU. At first glance, one might expect these rotations to be non-optimal since thrust is being “wasted” during several segments of the maneuver. However, the rotations of the spacecraft are due to the angular momentum accumulated during the initial part of the trajectory.

CONCLUSIONS

Including the attitude control requirement in the cost functional for optimal orbit transfers can have significant effects on the orbital maneuver performance. This paper presents an initial exploration of coupled orbit and attitude control for optimal orbit transfers and identifies several interesting types of trajectories that arise. Furthermore, some observations that are relevant to point-mass orbit transfers are not applicable to the problems where the rigid body motion is included. In particular, the near-invariance identified in an earlier

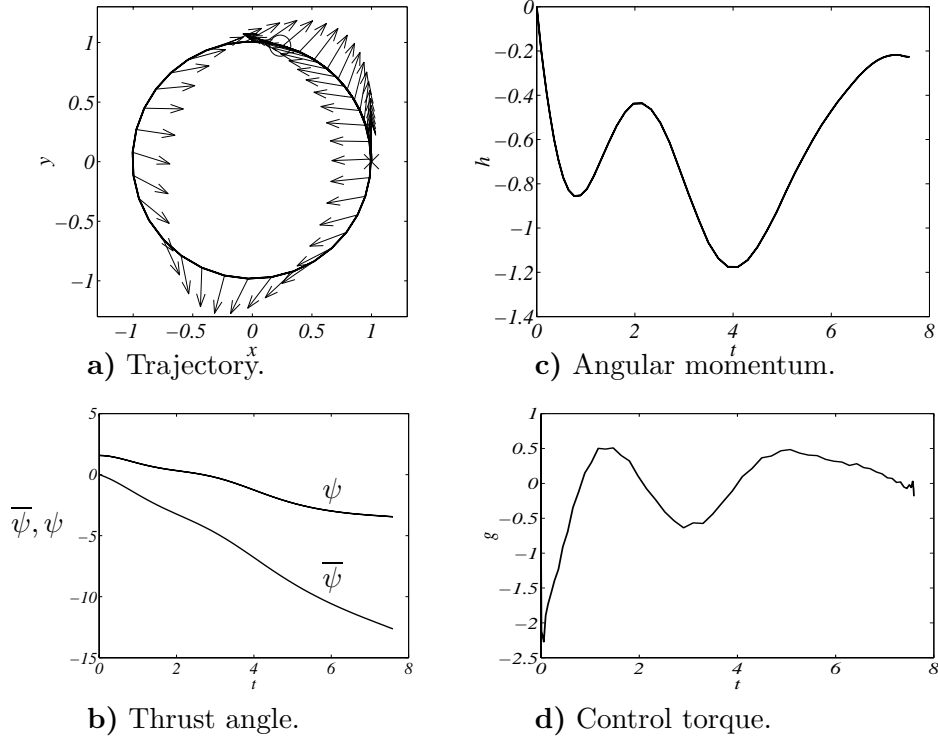


Figure 6: Trajectory, thrust angle, angular momentum, and control torque for Case B3.

work is seen to have less significance for this class of problems. The development presented in this paper allows the further investigation of this class of problems, with varying inertia, mass flow rates, and constraints on the control torque.

REFERENCES

- [1] LAWZEN, D. F., *Optimal Trajectories for Space Navigation*, Butterworths, London, 1963.
- [2] BRYSON, A. E., Jr. and HO, Y.-C., *Applied Optimal Control: Optimization, Estimation, and Control*, John Wiley & Sons, New York, 1975.
- [3] MAREC, J. P., *Optimal Space Trajectories*, Vol. 1 of *Studies in Astronautics* Elsevier, Amsterdam, 1979.
- [4] VINTER, R. B., *Optimal Control*, Birkhäuser, Boston, MA, 2000.
- [5] HAGER, W. W., “Runge-Kutta methods in optimal control and the transformed adjoint system,” *Numerische Mathematik*, Vol. 87, No. 2, 2000, pp. 247–282.
- [6] STRIZZI, J., ROSS, I. M., and FAHROO, F., “Towards Real-Time Computation of Optimal Controls for Nonlinear Systems,” In *Proceedings of the AIAA Guidance, Navigation and Control Conference*, Monterey, CA, August 2002.

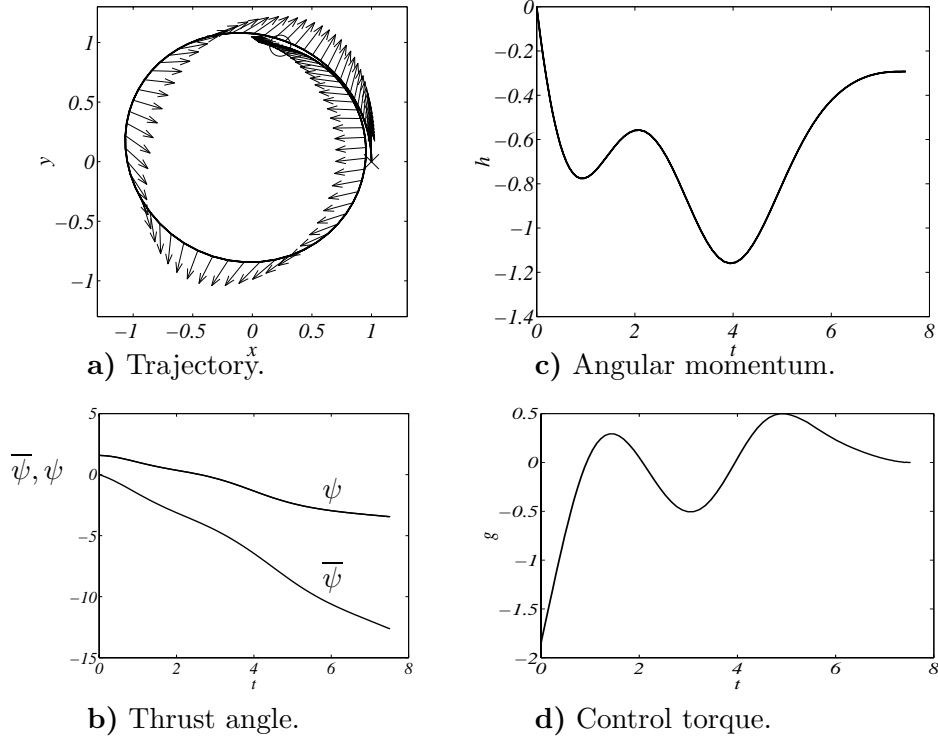


Figure 7: Trajectory, thrust angle, angular momentum, and control torque for Case A2.

- [7] ROSS, I. M., FAHROO, F., and STRIZZI, J., “Adaptive Grids for Trajectory Optimization by Pseudospectral Methods,” In *AAS/AIAA Spaceflight Mechanics Conference*, Ponce, Puerto Rico, February 2003.
- [8] JO, J.-W. and PRUSSING, J. E., “Procedure for Applying Second-Order Conditions in Optimal Control Problems,” *Journal of Guidance, Control and Dynamics*, Vol. 23, No. 2, 2000, pp. 241–250.
- [9] YAN, H., FAHROO, F., and ROSS, I., “Real-Time Computation of Neighboring Optimal Control Laws,” In *Proceedings of the AIAA Guidance, Navigation and, Control Conference*, Monterey, CA, August 2002.
- [10] THORNE, J. D. and HALL, C. D., “Minimum-Time Continuous-Thrust Orbit Transfers,” *Journal of the Astronautical Sciences*, Vol. 45, No. 4, 1997, pp. 411–432.
- [11] ALFANO, S. and THORNE, J. D., “Constant-Thrust Orbit-Raising,” *Journal of the Astronautical Sciences*, Vol. 42, No. 1, 1994, pp. 35–45.
- [12] THORNE, J. D. and HALL, C. D., “Approximate Initial Lagrange Costates for Continuous Thrust Spacecraft,” *Journal of Guidance, Control and Dynamics*, Vol. 19, No. 2, 1996, pp. 283–288.

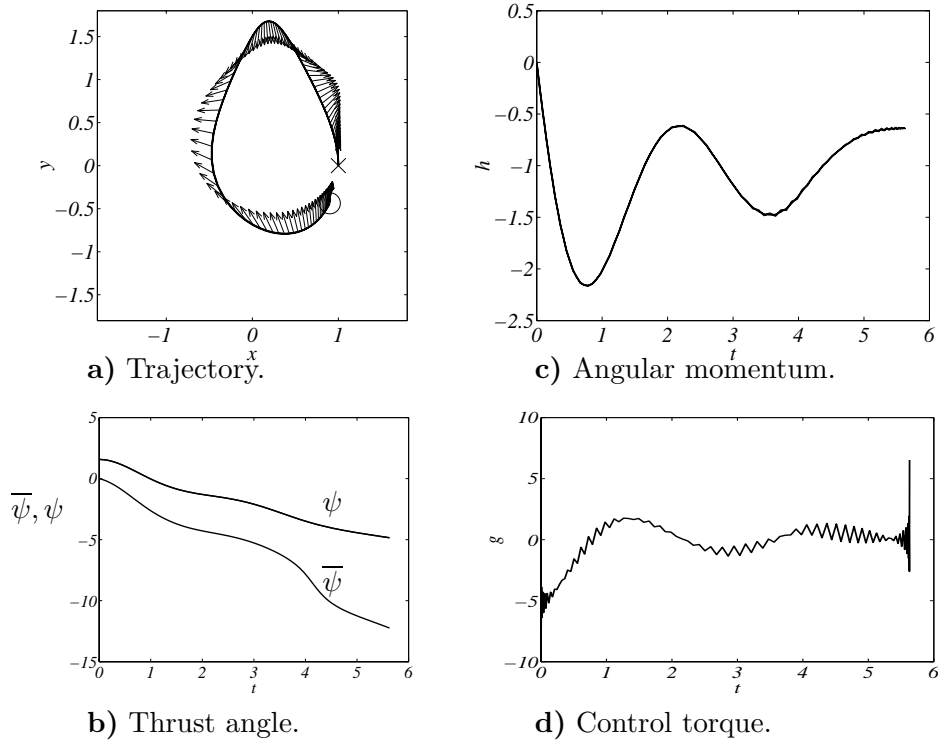


Figure 8: Trajectory, thrust angle, angular momentum, and control torque for Case D1.

- [13] MARASCH, M. W. and HALL, C. D., “Application of Energy Storage to Solar Electric Propulsion Orbital Transfer,” *Journal of Spacecraft and Rockets*, Vol. 37, No. 5, 2000, pp. 645–653.
- [14] HUGHES, S. P. and HALL, C. D., “Optimal Configurations for Rotating Spacecraft Formations,” *Journal of the Astronautical Sciences*, Vol. 48, No. 2–3, 2000, pp. 225–247.
- [15] CAMPBELL, M., FULLMER, R. R., and HALL, C. D., “The ION-F Formation Flying Experiments,” In *Proceedings of the 2000 AAS/AIAA Space Flight Mechanics Meeting*, Clearwater, Florida, Jan 2000.
- [16] ROSS, I. M., KING, J. T., and FAHROO, F., “Designing Optimal Spacecraft Formations,” In *Proceedings of the AIAA/AAS Astrodynamics Conference*, Monterey, CA, August 2002.
- [17] NAASZ, B. J., KARLGAARD, C. D., and HALL, C. D., “Application of Several Control Techniques for the Ionospheric Observation Nanosatellite Formation,” In *Proceedings of the 2002 AAS/AIAA Space Flight Mechanics Meeting*, San Antonio, Texas, Jan 2002.
- [18] NAASZ, B. J. Classical Element Feedback Control for Spacecraft Orbital Maneuvers. Master’s thesis, Virginia Polytechnic Institute and State University, Blacksburg, Virginia, 2002.

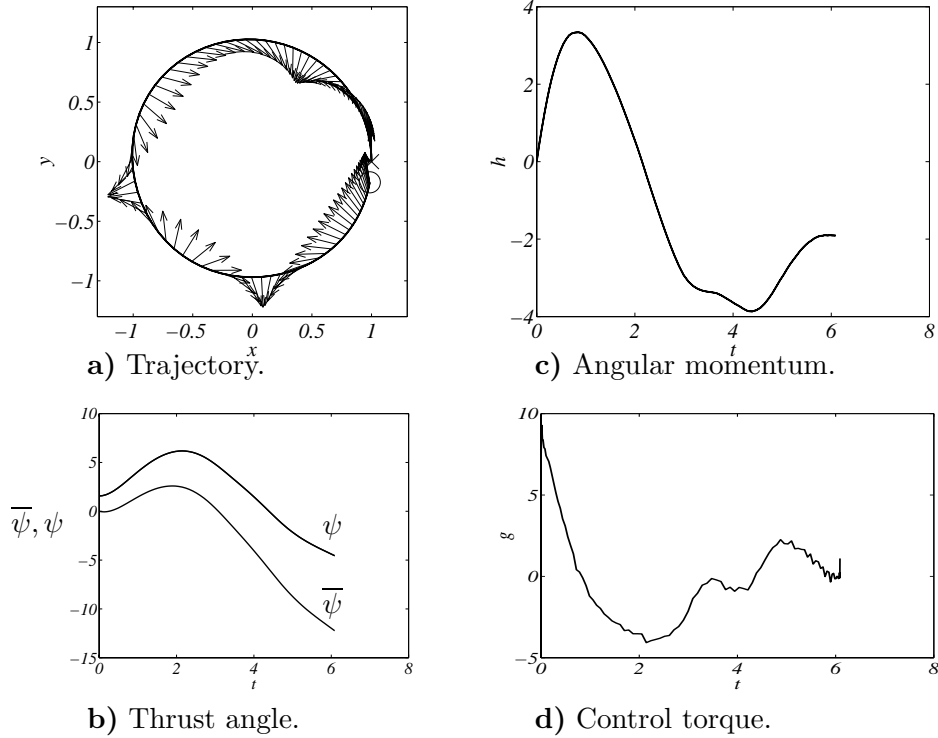


Figure 9: Trajectory, thrust angle, angular momentum, and control torque for Case D2.

- [19] NAASZ, B. J. and HALL, C. D., “Classical Element Feedback Control for Spacecraft Orbital Maneuvers,” *Journal of Guidance, Control and Dynamics*, 2003 (submitted)
- [20] ROSS, I. M. and FAHROO, F. User’s Manual for DIDO 2002: A MATLAB Application Package for Dynamic Optimization. Technical report, NPS Technical Report, AA-02-002, Department of Aeronautics and Astronautics, Naval Postgraduate School, Monterey, CA, June 2002.
- [21] ROSS, I. M. and FAHROO, F., *Legendre Pseudospectral Approximations of Optimal Control Problems*, Lecture Notes in Control and Information Sciences, Springer-Verlag (to appear)
- [22] BATE, R. R., MUELLER, D. D., and WHITE, J. E., *Fundamentals of Astrodynamics*, Dover, New York, 1971.
- [23] HALL, C. D. and COLLAZO PEREZ, V., “Minimum-Time Orbital Phasing Maneuvers,” *Journal of Guidance, Control and Dynamics*, 2003 (to appear)
- [24] STEVENS, R. and ROSS, I. M., “Preliminary Design of Earth-Mars Cyclers Using Solar Sails,” In *AAS/AIAA Spaceflight Mechanics Conference*, Ponce, Puerto Rico, February 2003.

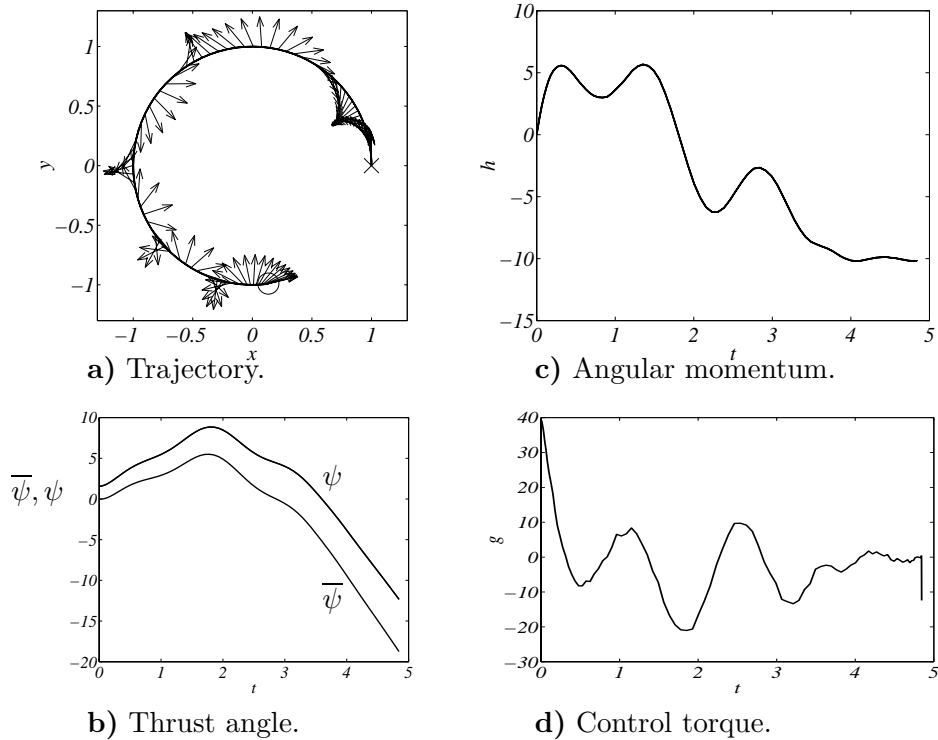


Figure 10: Trajectory, thrust angle, angular momentum, and control torque for Case D3.

- [25] FAHROO, F. and ROSS, I. M., “Costate estimation by a Legendre pseudospectral method,” *Journal of Guidance, Control and Dynamics*, Vol. 24, No. 2, 2001, pp. 270–277.
- [26] JOSSELYN, S. and ROSS, I. M., “A Rapid Verification Method for the Trajectory Optimization of Reentry Vehicles,” *Journal of Guidance, Control and Dynamics*, Vol. 26, No. 3, 2003 (to appear)
- [27] DENNIS, J. E., JR. and SCHNABEL, R. B., *Numerical Methods for Unconstrained Optimization and Nonlinear Equations*, Prentice-Hall, Englewood Cliffs, NJ, 1983.
- [28] SEYDEL, R., *From Equilibrium to Chaos: Practical Bifurcation and Stability Analysis*, Elsevier, New York, 1988.
- [29] BETTS, J. T., *Practical Methods for Optimal Control Using Nonlinear Programming*, Advances in Control and Design. SIAM, Philadelphia, 2001.
- [30] ROSS, I. M. and FAHROO, F., “A Perspective on Methods for Trajectory Optimization,” In *Proceedings of the AIAA/AAS Astrodynamics Conference*, Monterey, CA, August 2002.
- [31] ROSS, I. M., “Certain Connections in Optimal Control Theory and Computation,” In *Symposium on New Trends in Nonlinear Dynamics and Control and Their Applications*, Monterey, CA, October 2002.